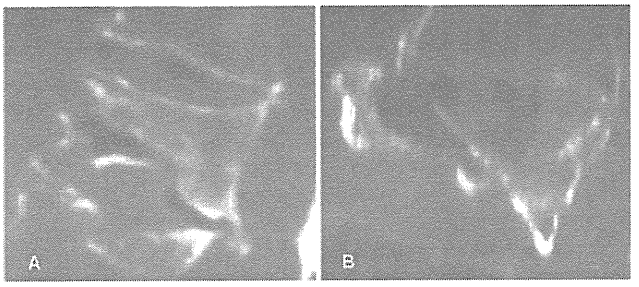

FIG. 6. Sagittal reconstructed CT scans showing communication of the air in the vertebra and the air in the adjacent intervertebral disc. A: Image obtained in a 67-year-old woman with an unhealed wedge-type fracture of the L-1 vertebra. The fluid sign in this case was negative. B: Image obtained in a 77-year-old woman with an unhealed wedge-type fracture of the L-3 vertebra. The fluid sign in this case was negative.

ous vertebroplasty. In our study group, all but 1 of the 14 patients with a positive fluid sign in an unhealed OVF had been hospitalized for pain and disability before referral to our institutions. In contrast, all 10 individuals with a negative fluid sign (air-filled) unhealed OVF were outpatients. Thus, the number of patients with the air-filled unhealed OVF is likely to be low in referral-based orthopedic clinics. Because patients with an air-filled unhealed OVF visit clinics with relatively mild back pain, it is important that they are not misdiagnosed. In fact, some of the patients in our study group had been treated for osteoporosis-related chronic back pain elsewhere before presenting to our institutions.

The presence of prevalent fractures may affect back pain status and performance status of patients with an acute OVF or an unhealed OVF. In this regard, frequency of the presence of prevalent fracture(s) was not significantly different between the patients with an unhealed OVF and those with an acute OVF (Table 1). Also, there was no significant difference in terms of frequency of prevalent fractures between unhealed OVFs with positive and negative fluid signs (Table 2). Patients who present for medical attention with back pain and have only a healed vertebral fracture may represent a suitable control group in the present study. However, in these patients, there is difficulty in determining whether healed OVF(s) are responsible for the pain symptoms.

Unhealed OVFs with small dynamic vertebral mobility may be treated successfully with the long-term wearing of a body jacket. However, in the literature, unhealed OVFs have been treated surgically rather than conservatively. A variety of surgical procedures have been reported for the treatment of unhealed OVFs. These include osteosynthesis,[9] decompression and fusion surgeries via anterior,[11,19] posterior,[12,19,25] and anteroposterior[27] approaches, percutaneous vertebroplasty,[2,10,23] and percutaneous kyphoplasty.[7] The treatment procedure was determined depending on the severity of the fracture and neurological compromise and the surgeon's preference. Whereas osteosynthesis and fusion surgeries aim at solid bone union for stabilization of the affected vertebra, union status following percutaneous vertebroplasty or percutaneous kyphoplasty has not yet been addressed.

Conclusions

Unhealed OVFs form a group of fractures that are distinct from acute OVFs regarding radiographic morphometry and contents of the intravertebral cleft. Dynamic fracture mobility serves as a primal pain determinant of patients with an unhealed OVF and potentially those with an acute OVF. Fluid accumulation in the intravertebral cleft in unhealed OVFs likely reflects the positioning of patients in daily activity.

Disclosure

The authors report no conflict of interest concerning the materials or methods used in this study or the findings specified in this paper.

Author contributions to the study and manuscript preparation include the following. Conception and design: Kawaguchi. Acquisition of data: Horigome, Yajima, Oda, Kii, Ida, Yoshimoto, Iba, Takebayashi. Analysis and interpretation of data: Kawaguchi, Horigome, Yajima, Oda. Drafting the article: Kawaguchi, Oda. Critically revising the article: Oda, Takebayashi. Reviewed final version of the manuscript and approved it for submission: all authors. Administrative/technical/material support: Horigome, Yajima, Oda, Kii, Ida, Yoshimoto, Iba, Takebayashi. Study supervision: Yamashita.

Acknowledgment

The authors thank Dr. M. Tamakawa for his support and comments on imaging analysis.

References

1. Bhalla S, Reinus WR: The linear intravertebral vacuum: a sign of benign vertebral collapse. **AJR Am J Roentgenol 170:** 1563–1569, 1998
2. Carlier RY, Gordji H, Mompoint DM, Vernhet N, Feydy A, Vallée C: Osteoporotic vertebral collapse: percutaneous vertebroplasty and local kyphosis correction. **Radiology 233:** 891–898, 2004
3. Dupuy DE, Palmer WE, Rosenthal DI: Vertebral fluid collection associated with vertebral collapse. **AJR Am J Roentgenol 167:**1535–1538, 1996
4. Eastell R, Cedel SL, Wahner HW, Riggs BL, Melton LJ III: Classification of vertebral fractures. **J Bone Miner Res 6:** 207–215, 1991
5. Freedman BA, Heller JG: Kummel disease: a not-so-rare complication of osteoporotic vertebral compression fractures. **J Am Board Fam Med 22:**75–78, 2009
6. Genant HK, Wu CY, van Kuijk C, Nevitt MC: Vertebral fracture assessment using a semiquantitative technique. **J Bone Miner Res 8:**1137–1148, 1993
7. Grohs JG, Matzner M, Trieb K, Krepler P: Treatment of intravertebral pseudarthroses by balloon kyphoplasty. **J Spinal Disord Tech 19:**560–565, 2006
8. Hasegawa K, Homma T, Uchiyama S, Takahashi H: Vertebral pseudarthrosis in the osteoporotic spine. **Spine 23:**2201–2206, 1998
9. Hasegawa K, Homma T, Uchiyama S, Takahashi HE: Osteosynthesis without instrumentation for vertebral pseudarthrosis in the osteoporotic spine. **J Bone Joint Surg Br 79:**452–456, 1997
10. Jang JS, Kim DY, Lee SH: Efficacy of percutaneous vertebroplasty in the treatment of intravertebral pseudarthrosis associated with noninfected avascular necrosis of the vertebral body. **Spine 28:**1588–1592, 2003
11. Kaneda K, Asano S, Hashimoto T, Satoh S, Fujiya M: The

treatment of osteoporotic-posttraumatic vertebral collapse using the Kaneda device and a bioactive ceramic vertebral prosthesis. **Spine 17 (8 Suppl):**S295–S303, 1992
12. Kim KT, Suk KS, Kim JM, Lee SH: Delayed vertebral collapse with neurological deficits secondary to osteoporosis. **Int Orthop 27:**65–69, 2003
13. Lafforgue P, Chagnaud C, Daumen-Legré V, Daver L, Kasbarian M, Acquaviva PC: The intravertebral vacuum phenomenon ("vertebral osteonecrosis"). Migration of intradiscal gas in a fractured vertebral body? **Spine 22:**1885–1891, 1997
14. Lane JI, Maus TP, Wald JT, Thielen KR, Bobra S, Luetmer PH: Intravertebral clefts opacified during vertebroplasty: pathogenesis, technical implications, and prognostic significance. **AJNR Am J Neuroradiol 23:**1642–1646, 2002
15. Linn J, Birkenmaier C, Hoffmann RT, Reiser M, Baur-Melnyk A: The intravertebral cleft in acute osteoporotic fractures: fluid in magnetic resonance imaging-vacuum in computed tomography? **Spine 34:**E88–E93, 2009
16. Malghem J, Maldague B, Labaisse MA, Dooms G, Duprez T, Devogelaer JP, et al: Intravertebral vacuum cleft: changes in content after supine positioning. **Radiology 187:**483–487, 1993
17. McKiernan F, Faciszewski T: Intravertebral clefts in osteoporotic vertebral compression fractures. **Arthritis Rheum 48:** 1414–1419, 2003
18. Mirovsky Y, Anekstein Y, Shalmon E, Peer A: Vacuum clefts of the vertebral bodies. **AJNR Am J Neuroradiol 26:**1634–1640, 2005
19. Mochida J, Toh E, Chiba M, Nishimura K: Treatment of osteoporotic late collapse of a vertebral body of thoracic and lumbar spine. **J Spinal Disord 14:**393–398, 2001
20. Oken MM, Creech RH, Tormey DC, Horton J, Davis TE, McFadden ET, et al: Toxicity and response criteria of the Eastern Cooperative Oncology Group. **Am J Clin Oncol 5:**649–655, 1982
21. Papaioannou A, Watts NB, Kendler DL, Yuen CK, Adachi JD, Ferko N: Diagnosis and management of vertebral fractures in elderly adults. **Am J Med 113:**220–228, 2002
22. Pappou IP, Papadopoulos EC, Swanson AN, Cammisa FP Jr, Girardi FP: Osteoporotic vertebral fractures and collapse with intravertebral vacuum sign (Kümmel's disease). **Orthopedics 31:**61–66, 2008
23. Peh WC, Gelbart MS, Gilula LA, Peck DD: Percutaneous vertebroplasty: treatment of painful vertebral compression fractures with intraosseous vacuum phenomena. **AJR Am J Roentgenol 180:**1411–1417, 2003
24. Resnick D, Niwayama G, Guerra J Jr, Vint V, Usselman J: Spinal vacuum phenomena: anatomical study and review. **Radiology 139:**341–348, 1981
25. Saita K, Hoshino Y, Kikkawa I, Nakamura H: Posterior spinal shortening for paraplegia after vertebral collapse caused by osteoporosis. **Spine 25:**2832–2835, 2000
26. Sarli M, Pérez Manghi FC, Gallo R, Zanchetta JR: The vacuum cleft sign: an uncommon radiological sign. **Osteoporos Int 16:**1210–1214, 2005
27. Suk SI, Kim JH, Lee SM, Chung ER, Lee JH: Anterior-posterior surgery versus posterior closing wedge osteotomy in posttraumatic kyphosis with neurologic compromised osteoporotic fracture. **Spine 28:**2170–2175, 2003
28. Yu CW, Hsu CY, Shih TT, Chen BB, Fu CJ: Vertebral osteonecrosis: MR imaging findings and related changes on adjacent levels. **AJNR Am J Neuroradiol 28:**42–47, 2007

Manuscript submitted April 28, 2009.
Accepted March 26, 2010.
Address correspondence to: Satoshi Kawaguchi, M.D., Department of Orthopaedic Surgery, Asahikawa Kosei Hospital, 111-3, 1-jo 24-chome, Asahikawa 078-8211, Japan. email: kawaguch@sapmed.ac.jp.

J Bone Miner Metab (2010) 28:561–567
DOI 10.1007/s00774-010-0164-5

ORIGINAL ARTICLE

Effects of raloxifene treatment on the structural geometry of the proximal femur in Japanese women with osteoporosis

Junichi Takada · Takami Miki · Yasuo Imanishi · Kiyoshi Nakatsuka · Hiroshi Wada · Hiroshi Naka · Takashi Yoshizaki · Kousuke Iba · Thomas J. Beck · Toshihiko Yamashita

Received: 20 November 2009 / Accepted: 24 January 2010 / Published online: 24 March 2010

Abstract The purpose of this study was to clarify the effects of 2-year treatment with raloxifene on the proximal femoral geometry among Japanese patients with osteoporosis by hip structure analysis. One hundred ninety-eight community-dwelling postmenopausal women with osteoporosis were enrolled. The structural variables were areal bone mineral density (BMD), cross-sectional area (CSA), section modulus (index of resistance to bending forces), and buckling ratio (index of cortical instability). BMD, CSA, and section modulus at the narrow neck significantly increased by 1.27, 2.67, and 3.90% at 2 years, respectively. BMD, CSA, and section modulus at the intertrochanter significantly increased by 2.55, 4.49, and 6.60% at study termination, respectively. The buckling ratio at the intertrochanter decreased by 2.36% at 1 year, but differences at 2 years became non-significant. Parameters at the shaft were qualitatively similar to those of the narrow neck and intertrochanter. The percent change of the section modulus was significantly higher than that of BMD at 2 years in all three regions. The percent changes of the section modulus is strongly correlated with the percent changes of BMD and CSA, and negative correlated with the percent changes of buckling ratio in all regions. In conclusion, Japanese osteoporotic women on raloxifene therapy have significant improvements of both BMD and geometry in the proximal femur.

Keywords Hip structure analysis · Raloxifene · Geometry · Bone strength · Hip fracture

J. Takada · K. Iba · T. Yamashita
Department of Orthopedic Surgery, Sapporo Medical University, Sapporo, Japan

J. Takada (✉) · T. Yoshizaki
Kitago Orthopedic Clinic, Sapporo, Japan
e-mail: jtakada@kitago-ortho.com

T. Miki · H. Naka
Department of Geriatrics, Osaka City University, Osaka, Japan

Y. Imanishi
Department of Metabolism, Endocrinology, and Molecular Medicine, Osaka City University Graduate School of Medicine, Osaka, Japan

K. Nakatsuka
Nozaki Clinic, Osaka, Japan

H. Wada
Wada Obstetrics and Gynecology Clinic, Asahikawa, Japan

T. J. Beck
Department of Radiology, The Johns Hopkins University, Baltimore, MD, USA

Introduction

Areal bone mineral density (BMD) measured by dual energy X-ray absorptiometry (DXA) is a valuable tool for the evaluation of bone fragility and shows significant correlations between BMD decline and risk of fracture [1–3]. However, BMD may not be the best assessment of treatment efficacy since the fracture reduction after treatment is only partially explained by increased BMD [4–6]. Strength of bone is however governed by structural dimensions and tissue materials properties, neither of which is directly measured by a conventional BMD measurement. Beck and Ruff have applied the hip structure analysis (HSA) method to measure proximal femur geometry and strength using conventional DXA scans of the hip [7, 8]. HSA has been

used to demonstrate age trends, racial and gender differences, and treatment effects on osteoporosis in Caucasians [8–16]. In Japan, we have previously demonstrated age-related differences in structural geometry and femoral strength and changing patterns in HSA geometry that may be consistent with the epidemiological evidence of hip fracture rates in Japan [17]. However, osteoporosis treatments analyzed by HSA have not previously been reported in Japanese patients.

The purpose of this study was to use the HSA method to gain some insights into the effects of a 2-year treatment with raloxifene on the proximal femur geometry among Japanese women with osteoporosis.

Materials and methods

One hundred ninety-eight community-dwelling, ambulatory, postmenopausal women were enrolled who had osteoporosis as defined by Japanese diagnostic criteria [18]. These criteria included low BMD (T score < -2.5) or presence of osteoporotic fractures. Patients with a history of hip fracture or any disease or medication known to affect bone metabolism were excluded from this study. All patients were given raloxifene (60 mg/day) over the study period.

DXA scans of the hip were taken at baseline, and were repeated at 6-, 12-, and 24-month follow-up points. Hip scans were performed using a hip positioner system (HPS; OsteoDyne, Durham, NC) to ensure consistent positioning [19]. This device keeps the subject's legs positioned in abduction and internal rotation (15°).

Hip structure analysis

The archived DXA images were analyzed using the HSA method, which has been described in detail in earlier publications [7, 8]. Briefly, DXA scan files were first converted into bone mass images in which pixel values represent bone mass in grams per square centimeter, using an automated program. The underlying principle of the method is that a line of pixels traversing the bone axis is a projection of the corresponding cross-section from which certain geometric properties can be derived.

Three measured sites were defined as (1) narrow neck, traversing the narrowest width of the femoral neck; (2) intertrochanter, along the bisector of the shaft and femoral neck axes; (3) shaft, at a distance of 1.5 times the minimum neck width, distal to the intersection of the neck and shaft axes.

The structural variables used in this paper were as follows [20, 21].

- Areal BMD (g/cm^2): mean values of BMD from the narrow neck region are on average about 14% higher than the conventional Hologic neck ROI values on the same subjects, although age trends were similar in previous reports [10].
- Outer diameter (cm): the distance between (blur corrected) outer margins of the cross-section.
- Cross-sectional area (CSA, cm^2): this is defined as the surface area of bone tissue in the cross-section after excluding soft tissue (marrow) spaces. CSA is an index of resistance to forces directed along the long axis of the bone.
- Section modulus (cm^3): this is an index of resistance to bending forces and is calculated as CSMI/d_{max} where CSMI is the cross-sectional moment of inertia and d_{max} is the maximum distance from either bone edge to the centroid of the profile.
- Average cortex (cm): this is an estimate of the mean cortical thickness assuming a circular (narrow neck or shaft) or elliptical (intertrochanter) annulus model of the cross-section for use in the estimated buckling ratio. The model assumes that 60, 70, and 100% of the measured bone mass is in the cortex for the narrow neck, intertrochanter and shaft, respectively.
- Buckling ratio: this describes stable configurations of thin-walled tubes subjected to compressive loads and is estimated as the ratio of d_{max} to the estimated mean cortical thickness.

In addition to these parameters, the HSA program measures neck-shaft angle and femoral-neck length. The latter is defined as the distance from the center of the femoral head to the intersection of the neck and shaft axes.

Statistical analysis

All parameters are presented as mean (standard deviations, SD) at baseline and percent differences from baseline (95% confidence interval, CI). Differences were regarded as statistically significant when the 95% CI did not include zero. P values from two-sample t tests were employed to compare HSA parameter means. The correlations between HSA parameters were analyzed by Pearson's R and considered statistically significant at $P < 0.05$.

Results

Clinical characteristics at baseline

The mean (SD) age, body mass index, neck shaft angle, and neck length were 62.6 (7.7) years, 22.0 (3.0) kg/m^2, 129.1

(4.6) degrees, and 4.7 (0.5) cm, respectively. The neck-shaft angles and femoral-neck lengths were not significantly different from Japanese values (neck-shaft angle: 129.9°, femoral-neck length: 4.7 cm) from our previous report [17].

Changes from baseline in HSA parameters over 2 years

Based on repeated measures analyses, the baseline values and the percent changes from baseline in each parameter are shown in Tables 1, 2, and 3.

Narrow neck

BMD significantly increased by 1.27% (95% CI: 0.01, 2.54) compared to baseline at 2 years. The section modulus, an index of bending strength, significantly increased by 2.53% (95% CI: 1.22, 3.85) and 3.90% (95% CI: 2.33, 5.47) compared to baseline at 1 and 2 years, respectively. Compared to baseline, the mean difference in CSA was 1.20% (95% CI: 0.32, 2.08) after 1 year and 2.67% (95% CI: 1.44, 3.90) at study termination. Outer diameter significantly increased at study termination; however, changes in average cortex and buckling ratio did not reach significance (Table 1).

Intertrochanter

BMD increased significantly by 2.73% (95% CI: 1.88, 3.58) at 1 year and then remained relatively constant thereafter by 2.55% (95% CI: 1.55, 3.55) at study termination. The section modulus significantly increased by 4.63% (95% CI: 3.38, 5.87) and 6.60% (95% CI: 4.93, 8.26) compared to baseline at 1 and 2 years, respectively. The buckling ratio decreased by 2.36% (95% CI: −3.55, −1.16) at 1 year, but differences at 2 years became non-significant (−0.69%, 95% CI; −2.05, 0.66). The other parameters, CSA, outer diameter, and average cortex, were all significantly increased at study termination by 4.49% (95% CI: 3.30, 5.67), 1.92% (95% CI: 1.07, 2.78), and 2.78% (95% CI: 1.44, 4.12), respectively (Table 2).

Shaft

Results at the femoral shaft were qualitatively similar to those of the narrow neck and intertrochanter. The effects of raloxifene were significantly increased in all parameters except buckling ratio at study termination (Table 3).

It is worth noting that the % change of the section modulus was significantly higher than that of BMD at 2 years in all three regions.

Table 1 Mean (SD) bone values at baseline and mean percent difference (95% CI) from baseline in raloxifene treatment in 2 years at the narrow neck region

Narrow neck	Baseline values, mean (SD)	% difference vs. baseline, mean (95% CI)		
		6 months	12 months	24 months
BMD (g/cm^2)	0.742 (0.134)	0.03 (−0.81, 0.87)	0.47 (−0.50, 1.45)	1.27 (0.01, 2.54)*
CSA (cm^2)	2.033 (0.351)	0.89 (−0.14, 1.92)	1.20 (0.32, 2.08)*	2.67 (1.44, 3.90)*
Outer diameter (cm)	2.889 (0.186)	0.85 (0.39, 1.30)*	0.81 (0.25, 1.36)*	1.44 (0.68, 2.20)*
Section modulus (cm^3)	0.875 (0.165)	1.68 (0.14, 3.22)*	2.53 (1.22, 3.85)*	3.90 (2.33, 5.47)*
Average cortex (cm)	0.142 (0.027)	0.00 (−0.89, 0.89)	0.51 (−0.53, 1.55)	1.28 (−0.06, 2.61)
Buckling ratio	11.601 (0.118)	1.72 (0.61, 2.84)*	1.38 (−0.41, 3.17)	0.56 (−1.73, 2.81)

* $P < 0.05$ vs. baseline

Table 2 Mean (SD) bone values at baseline and mean percent difference (95% CI) from baseline in raloxifene treatment in 2 years at the intertrochanter region

Intertrochanter	Baseline values, mean (SD)	% difference vs. baseline, mean (95% CI)		
		6 months	12 months	24 months
BMD (g/cm^2)	0.749 (0.134)	2.12 (1.53, 2.87)*	2.73 (1.88, 3.58)*	2.55 (1.55, 3.55)*
CSA (cm^2)	3.507 (0.593)	2.15 (1.36, 2.94)*	3.53 (2.64, 4.41)*	4.49 (3.30, 5.67)*
Outer diameter (cm)	4.937 (0.343)	−0.02 (−0.56, 0.52)	0.82 (0.24, 1.41)*	1.92 (1.07, 2.78)*
Section modulus (cm^3)	2.903 (0.552)	2.29 (1.22, 3.36)*	4.63 (3.38, 5.87)*	6.60 (4.93, 8.26)*
Average cortex (cm	0.305 (0.059)	2.50 (1.65, 3.36)*	3.24 (2.15, 4.33)*	2.78 (1.44, 4.12)*
Buckling ratio	9.510 (2.346)	−2.38 (−3.20, −1.56)*	−2.36 (−3.55, −1.16)*	−0.69 (−2.05, 0.66)

* $P < 0.05$ vs. baseline

Table 3 Mean (SD) bone values at baseline and mean percent difference (95% CI) from baseline in raloxifene treatment in 2 years at the shaft region

Shaft	Baseline values, mean (SD)	% difference vs. baseline, mean (95% CI)		
		6 months	12 months	24 months
BMD (g/cm^2)	1.258 (0.218)	1.33 (0.65, 2.00)*	1.77 (0.89, 2.66)*	1.80 (0.76, 2.84)*
CSA (cm^2)	3.284 (0.527)	1.18 (0.48, 1.87)*	2.27 (1.43, 3.10)*	3.54 (2.48, 4.59)*
Outer diameter (cm)	2.754 (0.182)	−0.14 (−0.43, 0.15)	0.54 (0.07, 1.00)*	1.74 (1.18, 2.31)*
Section modulus (cm^3)	1.693 (0.312)	0.47 (−0.51, 1.45)	2.56 (1.36, 3.77)*	4.74 (3.26, 6.23)*
Average cortex (cm)	0.465 (0.105)	1.81 (0.92, 2.71)*	2.44 (1.12, 3.75)*	2.08 (0.62, 3.55)*
Buckling ratio	3.234 (0.919)	−1.59 (−2.60, −0.58)*	−1.26 (−2.79, 0.28)	0.11 (−1.55, 1.78)

* $P < 0.05$ vs. baseline

Table 4 Cross-correlations (Pearson's R) among the percent changes of parameters in hip structure analysis at the narrow neck region

Narrow neck	BMD	CSA	Outer diameter	Section modulus	Average cortex	Buckling ratio
BMD	1.000	0.840**	−0.465**	0.794**	0.998**	−0.862**
CSA		1.000	0.084	0.797**	0.825**	−0.520**
Outer diameter			1.000	−0.172*	−0.486**	0.769**
Section modulus				1.000	0.785**	−0.648**
Average cortex					1.000	−0.869**
Buckling ratio						1.000

* $P < 0.05$, ** $P < 0.001$

Table 5 Cross-correlations (Pearson's R) among the percent changes of parameters in hip structure analysis at the intertrochanteric region

Intertrochanter	BMD	CSA	Outer diameter	Section modulus	Average cortex	Buckling ratio
BMD	1.000	0.761**	−0.297**	0.535**	0.714**	−0.837**
CSA		1.000	0.392**	0.879**	0.894**	−0.708**
Outer diameter			1.000	0.534**	0.302**	0.148
Section modulus				1.000	0.757**	−0.557**
Average cortex					1.000	−0.868**
Buckling ratio						1.000

** $P < 0.001$

Table 6 Cross-correlations (Pearson's R) among the percent changes of parameters in hip structure analysis at the shaft region

Shaft	BMD	CSA	Outer diameter	Section modulus	Average cortex	Buckling ratio
BMD	1.000	0.865**	−0.360**	0.628**	0.975**	−0.909**
CSA		1.000	0.155	0.856**	0.803**	−0.598**
Outer diameter			1.000	0.357**	−0.416**	0.682**
Section modulus				1.000	0.561**	−0.361**
Average cortex					1.000	−0.914**
Buckling ratio						1.000

** $P < 0.001$

Correlations among the percent changes of parameters

Tables 4, 5, and 6 show correlations (Pearson's R) among the percent changes of HSA parameters in the narrow neck, intertrochanter, and shaft, respectively. The percent change of the section modulus is strongly correlated with the percent change of BMD, CSA, and average cortex and negatively correlated with the percent change of the

buckling ratio in all regions. As expected, the percent change of BMD has a positive relationship with the percent change of CSA, but a negative relationship with the percent change of outer diameter in all regions.

Discussion

One of the problems with the use of BMD as a monitor for osteoporosis treatment is that it does not completely capture the mechanical factors that lead to fragility [4–6]. On the other hand, bone geometry measurements have a more direct relationship with mechanical strength. In this study, we are the first to report that Japanese women on raloxifene therapy over 2 years had significant positive changes in the structural geometry at all measured cross sections of the proximal femur. Raloxifene treatment produced positive changes in CSA and in the section modulus, indices of geometric strength in axial compression and bending, respectively. These changes were particularly evident at the narrow neck and intertrochanter regions that correspond to common fracture sites. The interpretation of these data is complex because the interplay between structure and fragility is not completely understood.

It is critical to first consider the effect of periosteal expansion because it is a geometric confounder of BMD, but also opposing effects on bending resistance (section modulus) susceptibility. The expansion of bone outer diameters confounds conventional BMD analyses because it increases the region area over which the BMD is averaged (i.e., BMD = bone mineral content/region area). Thus, in general, any net gain in bone within cross sections due to treatment will be underestimated by BMD. This was the case in the present study as treatment-induced gain in bone (directly measured as CSA in HSA) is roughly twice that apparent in the BMD due to the effects of expansion (Tables 1, 2, 3). An increase in CSA will improve its resistance to the axial component of those loads. Under most conditions, however, bending dominates physiologic loads on the proximal femur, and addition of bone to the outer surface has a preferentially greater effect on the section modulus. In the present study, the treatment-induced effect on bending resistance (section modulus) is about 30–50% greater than the effect on CSA and 2–3 times the effect on BMD in the same region.

Outer diameters widened from baseline in all three femur regions, becoming significant after 12 months. Lack of a placebo group in the present study prevents drawing conclusions regarding treatment effects on expansion. The yearly changes of outer diameter in the present study were higher than that of literally reported data in untreated Japanese women (narrow neck: 0.46%/year, intertrochanter: 0.22%/year, shaft: 0.16%/year) [17]. However, it could not be concluded that the expansion of outer diameter in this study was the effect of raloxifene, because the literally reported data include not only osteoporotic patients, but also normal women, and the baseline values in this study were lower than those in literal data. In addition, the multiple outcomes of raloxifene evaluation (MORE) trial was unable to detect raloxifene effects on rates of periosteal apposition vs. placebo [12]. For the above-mentioned reasons, the expansion of outer diameter in the present study might mainly appear to accompany the aging process rather than the effects of raloxifene.

Nevertheless, the presence of expansion in the present study does have important implications because it modifies the effects of bone gain due to treatment. Although the outer diameter expands with age in untreated patients, average cortex, CSA, and section modulus decrease with age. On the other hand, the average cortex, CSA, and section modulus in raloxifene treatment were significantly increased. These results indicated that raloxifene decreased the bone resorption in endocortical bone without inhibiting the bone formation in periosteal, and induced an increase in the average cortex, CSA and section modulus.

Our results in Japanese women were generally consistent with the larger MORE study of raloxifene effects on a mostly (95.7%) white population of postmenopausal women with osteoporosis [12] with one notable difference. In both studies, significant improvements (reduction) in buckling ratios were evident at the narrow neck and intertrochanter regions at early time points, but differences declined with time. In the MORE study, a 2% lower buckling ratio remained significant at 3 years [12], but in our study, the buckling ratios were no longer significant after 2 years of treatment. A clinical trial by Greenspan et al. [13] evaluated the effects of estrogen replacement therapy on femur geometry, and showed positive effects on CSA and section modulus that were comparable to those of the present study. Interestingly, after 3 years of estrogen treatment, there were no apparent differences from baseline in buckling ratio at the narrow neck, intertrochanter, and shaft regions. Treatments followed for longer periods seem to initially reduce the buckling ratio, but with continued expansion the effect seems to moderate with time [12, 16, 22]. This mechanism still needs to be carefully studied.

MORE and the present study showed significantly improved geometric parameters in the proximal femur, which were similar to those of alendronate, risedronate, and estrogen, so that the important question is whether these results lead to a reduction of the incidence of hip fracture. In previous clinical trials, alendronate, risedronate, and estrogen have shown protective effects against hip fracture, but there are no reports about raloxifene for the reduction of hip fractures [23–28]. Alendronate, risedronate, and raloxifene (MORE) significantly improved

both the section modulus and buckling ratio, and the results for estrogen and the present study have shown significantly increased section modulus. These data indicated that there is no qualitative difference in the changes of geometric parameters (section modulus, buckling ratio) between raloxifene and others (alendronate, risedronate, estrogen). On the other hand, alendronate significantly improved the section modulus and buckling ratio compared to risedronate in a head-to-head trial [15]. However, these quantitative differences could not directly explain the risk reduction of hip fracture, because there is no evidence that alendronate has a superior effect for reducing hip fracture compared to risedronate. The quantitative differences between raloxifene and others (alendronate, risedronate, and estrogen) could not explain the risk reduction of hip fracture, because there is no head-to-head comparison study.

The MORE trial has shown that raloxifene treatments reduce new vertebral fracture incidence by about half compared to placebo control [23, 24], but the incidence of hip fracture in that trial was inadequate to detect effects on hip fracture rates. This contrasts with the alendronate (FIT-1) and risedronate (HIP) studies, where because of differences in enrollment criteria, rates of hip fracture in control groups were 3–5 times higher in the FIT-1 (2.2%) and HIP (3.2%) studies vs. 0.7% in MORE [23, 25, 26]. Nakamura et al. [29] reported that raloxifene treatment at 60 mg/day for 1 year resulted in a significant reduction in the risk of new clinical vertebral fractures and any new clinical fracture in postmenopausal Asian women with osteoporosis. Moreover, in a recent observational study, there were no significant differences in hip fracture incidence between patients treated with risedronate, raloxifene, and alendronate [30]. Raloxifene may reduce the incidence of hip fracture as well as risedronate and alendronate, although this would be difficult to prove in a head-to-head study because of the low incidence of hip fracture and the necessity for enrolling huge numbers of patients.

There are methodological limitations to our study; DXA scanners are not designed or optimized to measure structural dimensions. Precision, not evaluated in the present study, was relatively poor in the MORE study [12]. The main reason is the difficulty in reproducing the position of the three-dimensional femur in two-dimensional images separated months to years apart. Imprecision may prevent the detection of subtle effects on geometry in this study. In addition, use of two-dimensional DXA scans means that the section modulus is assessed only in the scan plane; effects of treatment may be different for bending directions out of the image plane.

Although there were some limitations, this study also has significant strengths. This is the first study employing the HSA method to examine geometric strength-related parameters in elderly Japanese women on raloxifene therapy over 2 years. Although these women maintained their hip BMD, there were statistically significant changes in the underlying geometry that have not previously been reported in this population. It is clear that like other osteoporosis treatments, raloxifene alters femur geometry in a positive direction. If technological improvements can make them reliable enough for clinical use, geometric measurements may ultimately provide a clearer view of the pharmacological efficacy of osteoporosis treatments.

We conclude that Japanese women on raloxifene therapy have significant improvements of both BMD and proximal hip structural geometry. Women who were treated with raloxifene showed positive structural changes in the proximal regions of the femur that suggest improved bending and axial strength over 2 years.

Acknowledgments The authors wish to acknowledge Mr. Etsuro Hamaya of Eli Lilly & Co. Lilly Research Laboratories, Japan, for his assistance.

References

1. Kanis JA (2002) Diagnosis of osteoporosis and assessment of fracture risk. Lancet 359:1929–1936
2. Miller PD (2003) Bone mass measurements. Clin Geriatr Med 19:281–297
3. Schott AM, Cormier C, Hans D, Favier F, Hausherr E, Dargent-Molina P, Delmas PD, Ribot C, Sebert JL, Breart G, Meunier PJ, EPIDOS Group (1998) How hip and whole-body bone mineral density predict hip fracture in elderly women: the EPIDOS prospective study. Osteoporos Int 8:247–254
4. Li Z, Meredith MP, Hoseyni MS (2001) A method to assess the proportion of treatment effect explained by a surrogate endpoint. Stat Med 20:3175–3188
5. Cummings SR, Karpf DB, Harris F, Genant HK, Ensrud K, LaCroix AZ, Dennis M, Black DM (2002) Improvement in spine bone density and reduction in risk of vertebral fractures during treatment with antiresorptive drugs. Am J Med 112:281–289
6. Sarkar S, Mitlak BH, Wong M, Stock JL, Black DM, Harper KD (2002) Relationships between bone mineral density and incident vertebral fracture risk with raloxifene therapy. J Bone Miner Res 17:1–10
7. Beck TJ, Ruff CB, Warden KE, Scott WW Jr, Rao GU (1990) Predicting femoral neck strength from bone mineral data: a structural approach. Investig Radiol 25:6–18
8. Beck TJ, Ruff CB, Scott WW Jr, Plato CC, Tobin JD, Quan CA (1992) Sex differences in geometry of the femoral neck with aging: a structural analysis of bone mineral data. Calcif Tissue Int 50:24–29
9. Beck TJ, Ruff CB, Bissessur K (1993) Age-related changes in female femoral neck geometry: implications for bone strength. Calcif Tissue Int 53:S41–S46
10. Beck TJ, Looker AC, Ruff CB (2000) Structural trends in the aging femoral neck and proximal shaft: analysis of the third national health and nutrition examination survey dual-energy X-ray absorptiometry data. J Bone Miner Res 15:2297–2304
11. Wang XF, Duan Y, Beck TJ, Seeman E (2005) Varying contributions of growth and ageing to racial and sex differences in femoral neck structure and strength in old age. Bone 36:978–986

12. Uusi-Rasi K, Beck TJ, Semanick LM, Daphtary MM, Crans GG, Desaiah D, Harper KD (2006) Structural effects of raloxifene on the proximal femur: results from the multiple outcomes of raloxifene evaluation trial. Osteoporos Int 17:575–586
13. Greenspan SL, Beck TJ, Resnick NM, Bhattacharya R, Parker RA (2005) Effect of hormone replacement, alendronate, or combination therapy on hip structure geometry: a 3-year, double blind, placebo-controlled clinical trial. J Bone Miner Res 20:1525–1532
14. Uusi-Rasi K, Semanick LM, Zanchetta JR, Bogado CE, Eriksen EF, Sato M, Beck TJ (2005) Effects of teriparatide [rh PTH (1–34)] treatment on structural geometry of the proximal femur in elderly osteoporotic women. Bone 36:948–958
15. Bonnick SL, Beck TJ, Cosman F, Hochberg MC, Wang H, de Papp AE (2009) DXA-based hip structural analysis of once-weekly bisphosphonate-treated postmenopausal women with low bone mass. Osteoporos Int 20:911–921
16. Beck TJ, Lewiecki EM, Miller PD, Felsenberg D, Liu Y, Ding B, Libanati C (2008) Effects of denosumab on the geometry of the proximal femur in postmenopausal women in comparison with alendronate. J Clin Densitom 11:351–359
17. Takada J, Beck TJ, Iba K, Yamashita T (2007) Structural trends in the aging proximal femur in Japanese postmenopausal women. Bone 41:97–102
18. Osteoporosis diagnostic criteria review committee: Japanese society for bone, mineral research (2001) Diagnostic criteria for primary osteoporosis: year 2000 revision. J Bone Miner Metab 19:331–337
19. Hans D, Duboeuf F, Schott AM, Horn S, Avioli LV, Drezner MK, Meunier PJ (1997) Effects of a new positioner on the precision of hip bone mineral density measurements. J Bone Miner Res 12:1289–1294
20. Ruff CB, Hayes WC (1983) Cross-sectional geometry of Pecos Pueblo femora and tibiae—a biomechanical investigation. I. Method and general patterns of variation. Am J Phys Anthropol 60:359–381
21. Melton LJ III, Beck TJ, Amin S, Khosla S, Achenbach SJ, Oberg AL, Riggs BL (2005) Contributions of bone density and structure to fracture risk assessment in men and women. Osteoporos Int 16:460–467
22. Chen Z, Beck TJ, Cauley JA, Lewis CE, LaCroix A, Bassford T, Wu G, Sherrill D, Going S (2008) Hormone therapy improves femur geometry among ethnically diverse postmenopausal participants in the Women's Health Initiative hormone intervention trials. J Bone Miner Res 23:1935–1945
23. Ettinger B, Black DM, Mitlak BH, Knickerbocker RK, Nickelsen T, Genant HK, Christiansen C, Delmas PD, Zanchetta JR, Stakkestad J, Glüer CC, Krueger K, Cohen FJ, Eckert S, Ensrud KE, Avioli LV, Lips P, Cummings SR, Multiple Outcomes of Raloxifene Evaluation Investigators (1999) Reduction of vertebral fracture risk in postmenopausal women with osteoporosis treated with raloxifene: results from a 3-year randomized clinical trial. JAMA 282:637–645
24. Delmas PD, Genant HK, Crans GG, Stock JL, Wong M, Siris E, Adachi JD (2003) Severity of prevalent vertebral fractures and the risk of subsequent vertebral and nonvertebral fractures: results from the MORE trial. Bone 33:522–532
25. Black DM, Cummings SR, Karpf DB, Cauley JA, Thompson DE, Nevitt MC, Bauer DC, Genant HK, Haskell WL, Marcus R, Ott SM, Torner JC, Quandt SA, Reiss TF, Ensrud KE, Fracture Intervention Trial Research Group (1996) Randomised trial of effect of alendronate on risk of fracture in women with existing vertebral fractures. Lancet 348:1535–1541
26. McClung MR, Geusens P, Miller PD, Zippel H, Bensen WG, Roux C, Adami S, Fogelman I, Diamond T, Eastell R, Meunier PJ, Wasnich RD, Greenwald M, Kaufman JM, Chesnut CH, Reginster JY (2001) Effect of risedronate on the risk of hip fracture in elderly women. N Engl J Med 344:333–340
27. Writing Group for the Women's Health Initiative Investigators (2002) Risks and benefits of estrogen plus progestin in healthy postmenopausal women: principal results from the women's health initiative randomized controlled trial. JAMA 288:321–333
28. The Women's Health Initiative Steering Committee (2004) Effects of conjugated equine estrogen in postmenopausal women with hysterectomy: the women's health initiative randomized controlled trial. JAMA 291:1701–1712
29. Nakamura T, Liu JL, Morii H, Huang QR, Zhu HM, Qu Y, Hamaya E, Thiebaud D (2006) Effects of raloxifene on clinical fractures in Asian women with postmenopausal osteoporosis. J Bone Miner Metab 24:414–418
30. Cadarette SM, Katz JN, Brookhart MA, Stümer T, Stedman MR, Solomon DH (2008) Relative effectiveness of osteoporosis drugs for preventing nonvertebral fracture. Ann Intern Med 148:637–646

骨粗鬆症に伴う痛みの治療

Treatment for pain associated with osteoporosis

特集

射場 浩介 IBA Kousuke
山下 敏彦* YAMASHITA Toshihiko

すべての医師のための骨粗鬆症診療ガイド2010 Key words 骨粗鬆症 腰背部痛 椎体骨折 骨性疼痛 ビスフォスフォネート

本邦における骨粗鬆症の有病率は，女性で24%，男性で5%であり，推定患者数は800万人を超える．主な臨床症候は，脆弱性骨折とそれに伴う疼痛・機能障害であり，骨粗鬆症患者の治療において骨折予防と疼痛改善が最も重要である[1]．今回は，骨粗鬆症に伴う痛みの治療について，腰背部痛を中心に概説する．

骨粗鬆症に伴う腰背部痛

骨粗鬆症に伴う腰背部痛には，①椎体骨折に伴う疼痛と，②骨粗鬆症自体の疼痛がある．前者はさらに，①椎体骨折による疼痛と，②脊柱変形に伴う慢性疼痛に分けられる．

1. 椎体骨折に伴う疼痛

1)椎体骨折による疼痛

椎体骨折を起こすほどの有害な機械的ストレスは，椎体とその周囲組織に分布する侵害受容器を刺激して急性疼痛を引き起こす．また，骨折部や周囲の損傷組織ではマクロファージなどの炎症性細胞が内因性発痛物質を放し，侵害受容器を興奮(excitation)・感作(sensitization)状態として急性・慢性疼痛を引き起こす．椎体骨折による疼痛は，骨癒合に伴い経時的に改善をする．一方，長期経過においても骨癒合を認めず，骨折部の不安定性を呈する椎体偽関節では，頑固な慢性疼痛を認める(図1)．当科における偽関節部組織の免疫組織学的検討では，炎症細胞浸潤や血管新生を認めた．脊柱の不安定性や椎体周囲の炎症などの要因が複合してポリモーダル受容器に作用し，頑固な腰背部痛をきたすものと推測された．

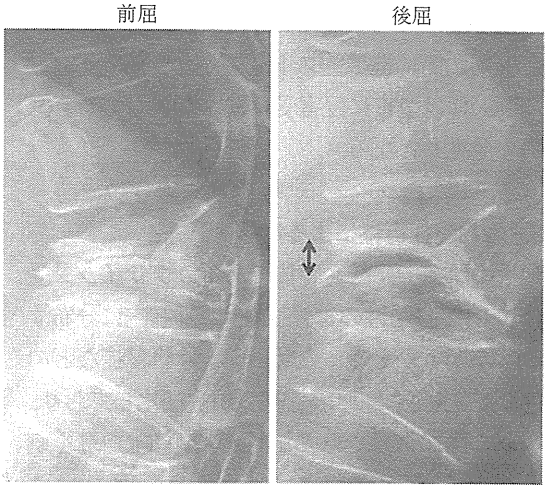

図1 第11胸椎椎体偽関節
椎体偽関節部は脊椎後屈で開大(矢印)を認める．

札幌医科大学医学部整形外科 講師 *教授

0371-1900/10/¥50/頁/JCOPY

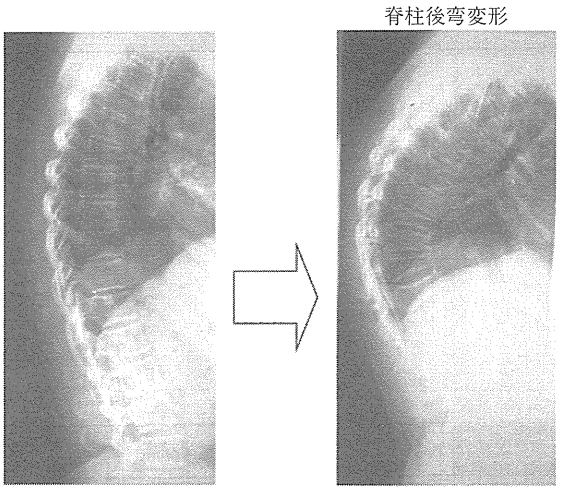

図2 多発性椎体骨折後に生じた脊柱後弯変形

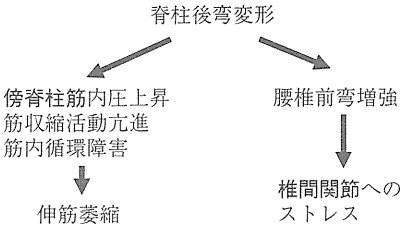

図3 脊柱後弯変形に伴う疼痛発生のメカニズム

2)脊柱変形に伴う疼痛

椎体骨折により胸腰椎の後弯変形が生じる(図2)と，傍脊柱筋の筋収縮活動が亢進するとともに，筋内圧が上昇する．さらに筋内循環障害，筋委縮が生じ，慢性腰痛の原因となる[2]．一方，胸椎後弯変形に対する腰椎の代償性前弯増強により，椎間関節に機械的ストレスがかかる(図3)．椎間関節には豊富に侵害受容器が存在しており，腰痛の発生源となる．

2. 骨粗鬆症自体による疼痛

最近の研究で，酸受容体であるカプサイシン受容体(TRPV1)陽性の神経線維[3]が骨髄内に分布することが明らかとなった(図4)．骨粗鬆症などの骨吸収亢進状態では，破骨細胞が活性化しており，骨吸収の際に形成される酸性環境がTRPV1を刺激して痛みを引き起こす[4]と考えられている(図5)．現在著者らは卵巣摘除(OVX)マウスを用

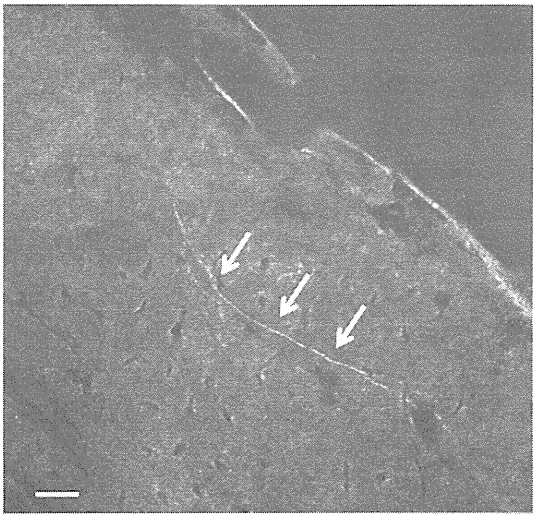

図4 抗TRPV1抗体による骨髄組織の免疫組織染色
TRPV1陽性の神経線維(白矢印)が骨髄内に分布することを確認した．(Niiyama, Kawamata, et al：unpublished data)

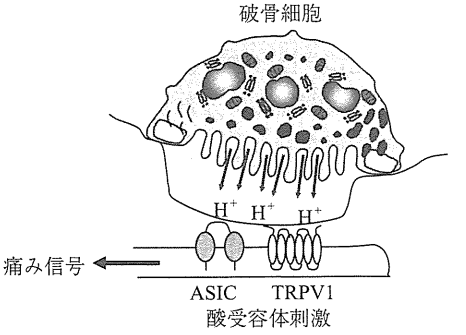

図5 破骨細胞が骨吸収時に形成する酸性環境が，骨髄内に分布する神経の酸受容体を刺激して痛み信号を発生する
(平賀 徹ほか：癌と骨病変(松本俊夫他編)，pp39-48，2004一部改変)

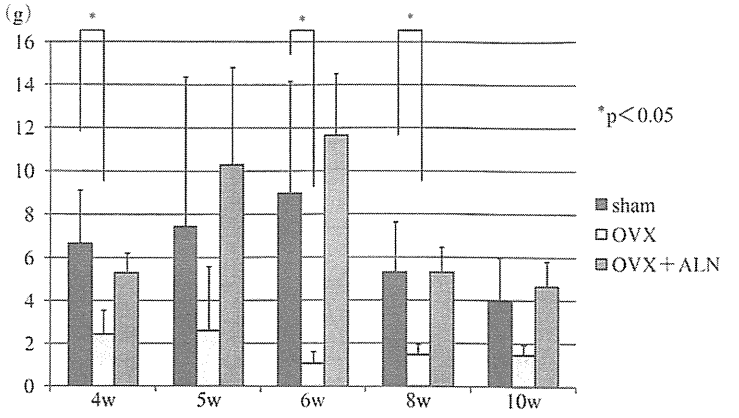

図6 OVX群はsham群と比較して疼痛域値の有意な低下を認め，さらにビスフォスフォネート投与で疼痛域値の改善を認めた
OVX後4，5，6，8，10週後にvon Frey testによる疼痛行動評価を行った．また，sham群，OVX後にビスフォスフォネートを投与した群(OVX＋ALN群)と疼痛域値を比較検討した．(Abe, et al：unpublished data)

いて，疼痛行動学的，免疫組織学的手法により，骨粗鬆症に伴う疼痛の発生メカニズムについて研究をすすめている．予備実験の段階ではあるが，疼痛行動学的検討においてOVXマウスは偽手術(sham)マウスと比較して疼痛閾値の低下を認めた．さらに，この低下した疼痛閾値は骨吸収抑制剤の投与で改善を認めた(図6)．このことは，骨粗鬆症に伴う疼痛の発生メカニズムを検討するうえで興味深い結果と考える．

骨粗鬆症に伴う痛みの治療

治療法には①薬物療法，②理学療法，③装具療法，④手術療法がある．疼痛を呈するそれぞれの病態に適した治療法の選択が必要となる．

1. 薬物療法

非ステロイド消炎鎮痛薬(NSAIDs)，ノイロトロピンや抗うつ薬(アミトリプチリンやタンドスピロン他)などの下行性疼痛抑制系賦活薬が用いられる．また，カルシトニンは破骨細胞の骨吸収を抑制する以外に，中枢性・末梢性の疼痛抑制効果を有することが知られている．

最近では，骨粗鬆症治療薬であるビスフォスフォネート(BP)や選択的エストロゲン受容体調節因子(SERM)が骨粗鬆症患者における腰背部痛を軽減することが報告されている[5]．これらの骨吸収抑制剤は，活性化した破骨細胞機能を抑制することで骨吸収亢進状態を改善する．そのため破骨細胞による酸性環境形成が障害され，酸受容体を介した疼痛刺激が減少する．以上のことが，BPやSERMが骨粗鬆症患者の疼痛を改善するメカニズムの1つとして考えられている．当科で行った検討でも，BP投与により骨粗鬆症患者の腰背部痛は有意に改善し，同時に骨吸収マーカーの低下を認めた(図7)．このことは骨吸収亢進状態を改善することが腰背部痛の改善に有用である可能性を示唆している．

2. 理学療法

物理療法として，温熱療法のホットパックや極超短波，電気療法としてTENSやSSP，レーザー治療などがあげられる．また，運動療法として，体幹筋力強化や全身的なストレッチングがすすめられる．

3. 装具治療

椎体骨折の急性期では疼痛改善と良好な骨癒合獲得のために，硬性・半硬性コルセット(図8)や体幹ギプスなどによる強固な外固定が重要であ

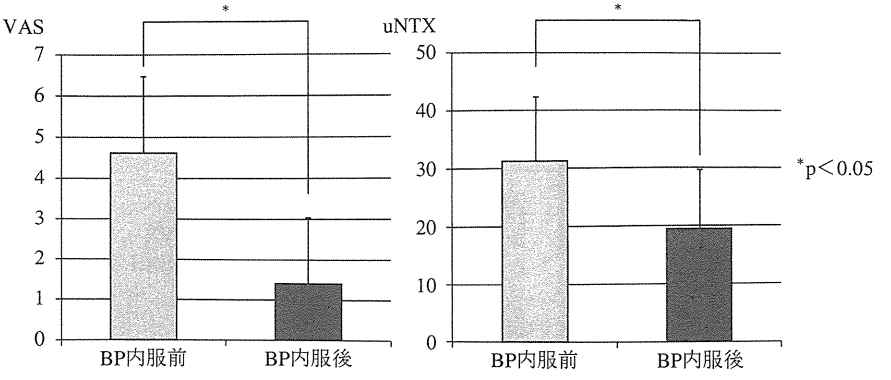

図7 骨粗鬆症に伴う腰背部痛に対するビスフォスフォネート(BP)の効果
腰背部痛は visual analogue scale(VAS)で評価を行い，骨代謝亢進状態の程度は尿中Ⅰ型コラーゲンN架橋テロペプチド(uNTX)で評価した．VASとuNTXはBP内服後に有意な低下を認めた．(当院骨粗鬆症外来での調査)

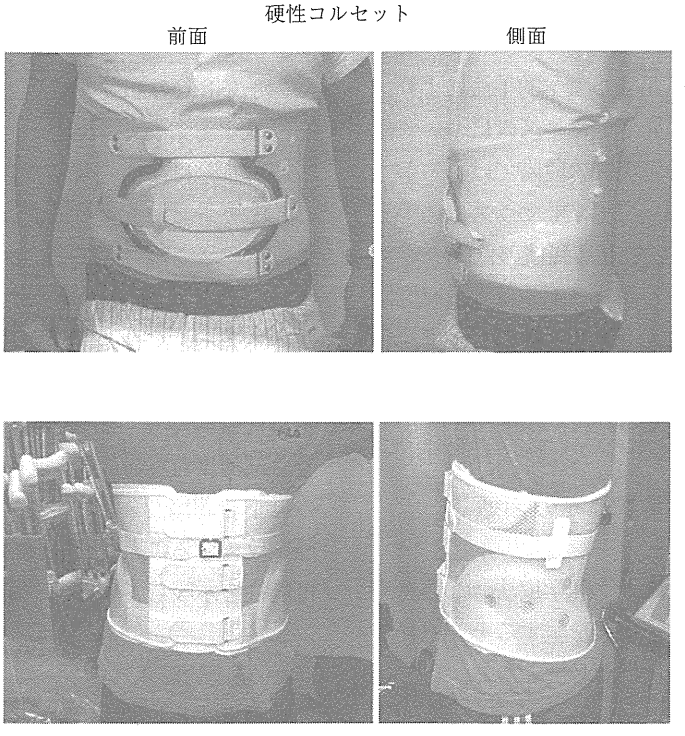

図8 硬性と半硬性コルセット

る．

4．手術治療

骨粗鬆症性椎体骨折後に遅発性神経障害を認める症例や，椎体偽関節部の不安定性を呈する症例では手術が適応となる．手術法には脊椎前方固定手術，後方固定手術，椎体形成術がある．経皮的椎体形成術は低侵襲手術であること，術後早期に疼痛が改善することから骨粗鬆症性椎体骨折後の偽関節症例に対して広く行われている(図9)．

5．慢性疼痛に対する治療

椎体骨折や脊柱変形を呈した症例のなかで，これまでに述べた治療で疼痛改善を認めない慢性疼

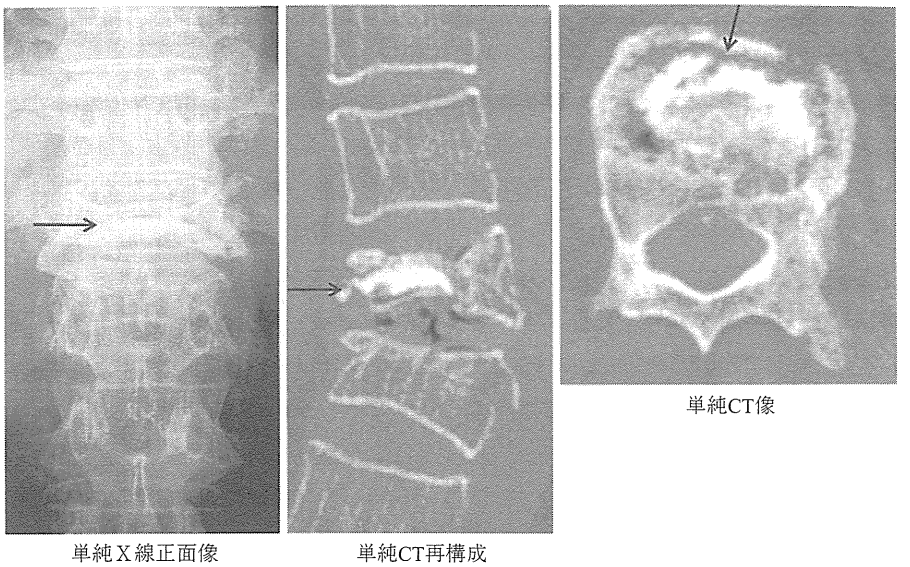

図9　第12胸椎椎体偽関節部に骨セメント(PMMA)を経皮的に注入(矢印)した
術後早期より腰背部痛は著明に改善した.

痛患者の治療は難渋する．このような症例では心理的，社会的要因が関与する場合があり，心理療法の併用や社会的ケアシステムの利用などの集学的治療の必要性も念頭に入れ，治療にあたることが重要である．

おわりに

骨粗鬆症に伴う腰背部痛の原因には，椎体骨折，偽関節，脊柱変形，骨吸収亢進など種々のものが考えられる．そのため，個々の病態を把握し，治療法を選択することが重要であると考える．

文　献
1) 骨粗鬆症の予防と治療ガイドライン作成委員会：骨粗鬆症の薬物治療．骨粗鬆症の予防と治療ガイドライン2006年度版，4-14，ライフサイエンス出版，東京，2006.
2) 熱田裕司，竹光正和，小林徹也ほか：姿勢異常と腰痛－筋原性疼痛の要素について－，骨・関節・靱帯　16：791-791，2003.
3) Mach DB, Rogers SD, Sabino MC, et al：Origins of skeletal pain：sensory and sympathetic innervation of mouse femur. Neruoscience 113：155-166, 2002.
4) Nagae M, Hiraga T, Wakabayashi H, et al：Osteoclasts play a part in pain due to the inflammation adjacent to bone. Bone 39：1107-1115, 2006.
5) 山崎　謙：リセドロネート投与による短期血清NTXの変化と腰痛の軽減効果の検討，Prog Med 24：1309-1315，2004.

骨組織における神経分布と痛み

射場 浩介*1) 山下 敏彦*2)

骨組織に分布する神経は，骨膜以外に皮質骨・海綿骨や骨髄腔内など広い範囲に存在する。神経線維では，有髄のAβ線維とAδ線維や無髄のC線維が確認されており，交感神経線維の分布も認めている。また，感覚神経終末端に存在する感覚受容器や神経終末より放出される神経ペプチドについても種々のものが骨組織内で確認されている。一方，これらの神経や感覚受容器，神経ペプチドの骨組織における役割についてはいまだに不明な点が多い。最近では，骨吸収亢進状態を呈する疾患で生じる疼痛は，破骨細胞活性化に伴う酸性環境が骨組織内に分布する酸受容体を介して侵害受容性神経を興奮させて生じることがわかってきた。今後，さらに研究が進み，骨組織における神経の役割について解明されていくことを期待する。

Control of bone remodeling by nervous system.

Nerve distribution and pain in bone tissue.

Department of Orthopaedic Surgery, Sapporo Medical University School of Medicine.

Kousuke Iba, Toshihiko Yamashita

The nerve fibers extensively innervate bone such as periosteum, compact and trabecular bone, and bone marrow space. Regarding as nerve fibers, there are myelinated fibers as Aβ and Aδ fibers, and unmyelinated fibers as C fiber, further, sympathetic nerve fibers also innervated bone tissue. In addition to nerve fibers, several receptors such as nociceptors at the terminal of the fibers, and released many kinds of neuropeptides were identified in the bone. On the other hand, most of roles concerning the nerve fibers, receptors and neuropeptides in bone were still unknown. Recently, bone pain of musculoskeletal disease is recognized to be related pathological condition at increasing bone resorption. It is thought to be a mechanism that a highly acidic condition at a bone compartment due to proton released from activated osteoclast stimulated acid sensing receptor as a nociceptor, and afferent signal induced bone pain.

*札幌医科大学医学部整形外科 1) 講師（いば・こうすけ） 2) 教授（やました・としひこ）

はじめに

骨の知覚は骨膜に分布する神経線維の受容器が刺激されたときにだけ生じ，骨皮質や骨髄には神経線維がないと考えられてきた[1]。しかし，その後の研究により知覚神経線維が骨内や骨髄内にも分布することが明らかとなってきた。また，外部刺激に対する入力末端装置である種々の感覚受容器も骨組織内の神経終末に存在することがわかってきた。本稿では，骨組織における神経線維や感覚受容器の分布について概説する。また，当教室で行っている骨性疼痛に関係する研究について紹介する。

神経線維と感覚受容器

知覚神経線維には，有髄のAα/β線維とAδ線維，無髄のC線維がある。主に，Aα/β線維は触覚・振動覚・深部覚を伝え，Aδ線維は鋭い痛み，C線維は鈍い痛みを伝える[2]。また，感覚神経線維の末梢端は種々の感覚受容器の形態をとる（**図1**）。感覚受容器には関節の位置や運動速度，靭帯や関節包への張力や圧を感知する固有感覚受容器（proprioceptor），“生体組織を損傷するか，あるいは損傷する可能性をもつ有害な刺激”である侵害刺激を感知する侵害受容器（nociceptor）がある[3]。固有感覚受容器はAα/βとAδ線維に支配される。侵害受容器は自由神経終末の形態をとり，Aδ線維とC線維に支配されている。この侵害受容器には機械的侵害刺激のみに反応する高域値機械受容器と，機械的刺激のほか化学的刺激や熱刺激にも反応するポリモーダル受容器（polymodal receptor）がある。とくに，ポリモーダル受容器は骨腫瘍や炎症疾患などで生じる骨組織への侵害受容に重要な役割をもつ[4][5]。ポリモーダル受容器の微細構造は，自由神経終末部に数百μmにわたるビーズ状の膨らみを呈し，その一部はシュワン鞘に覆われず基底膜が露出している[5][6]。この部分が受容器とされ，骨・骨膜組織や関節包に存在する[7]。また，侵害受容器は感覚の受容機能だけでなく効果器としての機能も有する。侵害受容器から有害信号が求心性に伝達されると，軸索反射によりほかの侵害受容線維末端から神経ペプチドが放出される。神経ペプチドには

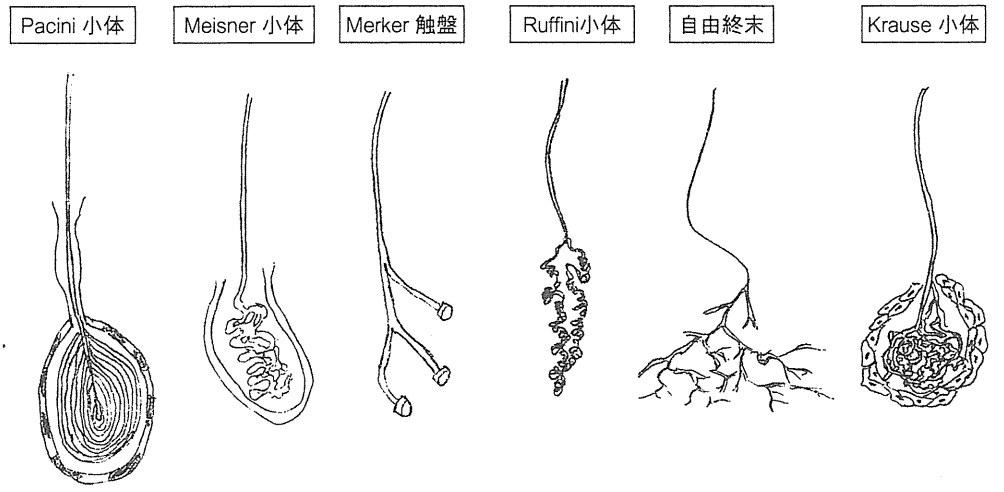

図1　知覚神経の感覚受容器

求心性神経終末の受容器には，嚢に包まれた球状あるいは錐状の形態をとるものや自由終末の形態をとるものがある。侵害受容器は自由神経終末の形態をとる。

（花岡一雄ほか改変）

サブスタンスP，ニューロキニンAおよびK，ソマトスタチン，**CGRP**（calcitonin gene related peptide），**VIP**（vasoactive intestinal poplypeptide）などがある。侵害受容器末梢組織に放出された神経ペプチドは，末梢血管拡張・透過性亢進，肥満細胞からのヒスタミン放出などの作用を及ぼし神経原性炎症を引き起こす[4]。いくつかの神経ペプチドは骨組織内で同定されており，神経線維や侵害受容器が機能していることを示している。

骨と神経分布

骨膜は神経，血管に富み，自由神経終末と固有感覚受容器のいずれも存在する。また，骨膜の表層や内層に疼痛関連の神経ペプチドであるサブスタンスP陽性の神経線維が同定されている[8]。

さらに骨基質や骨髄中にもハバース管やフォルクマン管を通じて神経が分布する。Aβ・Aδ線維C線維のいずれもが骨組織全体に広く分布している[9]（**図2**）。さらに，骨髄，骨皮質，骨膜にサブスタンスPやCGRP陽性の神経線維が同定されており[9)10)]（**図3**），筆者らの研究でもマウスの大腿骨骨髄内にCGRP陽性の神経線維を免疫組織染色で同定している（unpublished）。無髄神経の分布密度は骨膜が最も高いが，体積で考えた場合では骨髄腔に分布する神経が最も多いことが報告されている（**図4**）。また，皮質骨や海綿骨内の神経線維は，骨幹部と比較して近位・遠位骨端部に高密度に分布している。一方，骨髄腔では近位骨

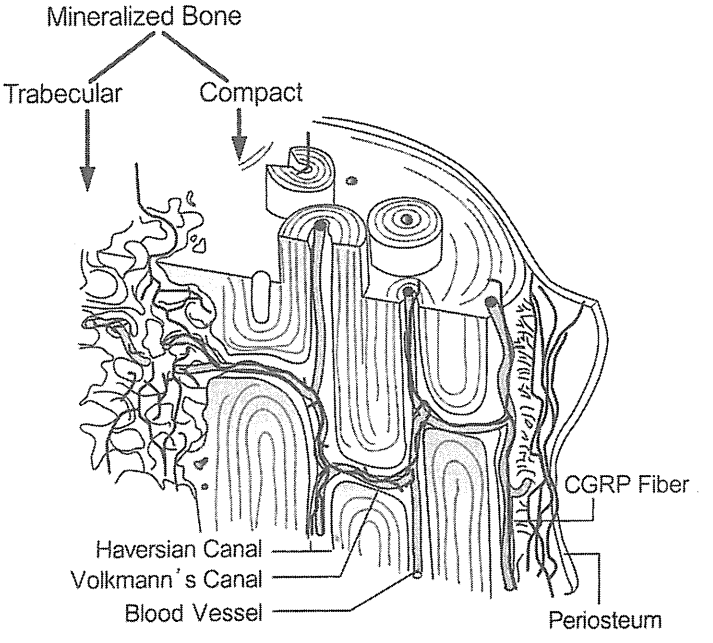

図2　骨膜から骨髄内への神経線維分布

骨の神経は骨周囲の骨膜からハバース管（Haversian Canal）やフォルクマン管（Volkmann's Canal）を通じて皮質骨（compact）や海綿骨（trabecular）内に分布する。

（文献9より改変引用）

CGRP：calcitonin gene related peptide，VIP：vasoactive intestinal poplypeptide

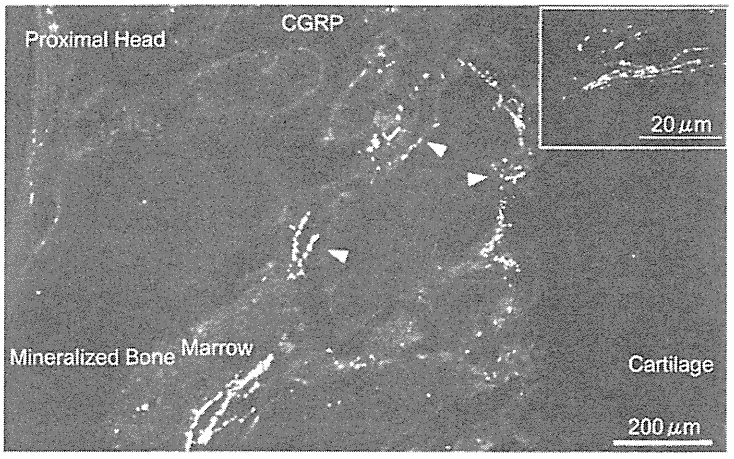

図3　マウス大腿骨近位端におけるCGRP陽性神経の分布

CGRP陽性神経線維が骨組織中に広く分していることがわかる。
Mineralized Bone：皮質骨＋海綿骨，Marrow：骨髄腔，Proximal Head：大腿骨近位骨端部，CGRP：calcitonin gene related peptide
（文献9より改変引用）

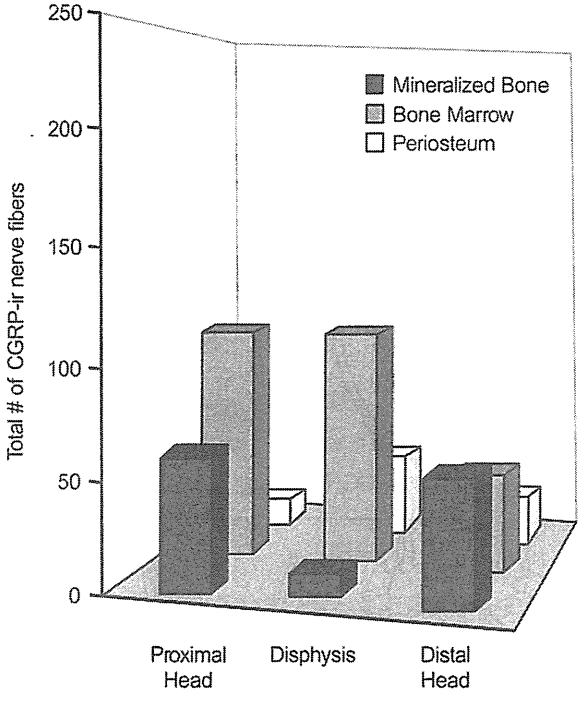

図4　単位体積あたりのCGRP陽性神経線維の分布体積

マウス大腿骨近位骨端部（Proximal Head），骨幹部（Diaphysis），遠位骨端部（Distal Head）におけるmm^3あたりのCGRP陽性神経線維が分布している体積。
Mineralized Bone：皮質骨＋海綿骨，Bone Marrow：骨以外の骨髄腔，Periosteum：骨膜，CGRP：calcitonin gene related peptide
（文献9，17より改変引用）

端部の神経分布密度が最も高く，骨幹部，遠位骨端部と続く（図4）。有髄神経の分布も同様の傾向を認めている[9]。

骨と交感神経系

交感神経は骨膜や骨組織に分布するとともに，骨組織内の血流や造血系細胞の分化や機能の調節

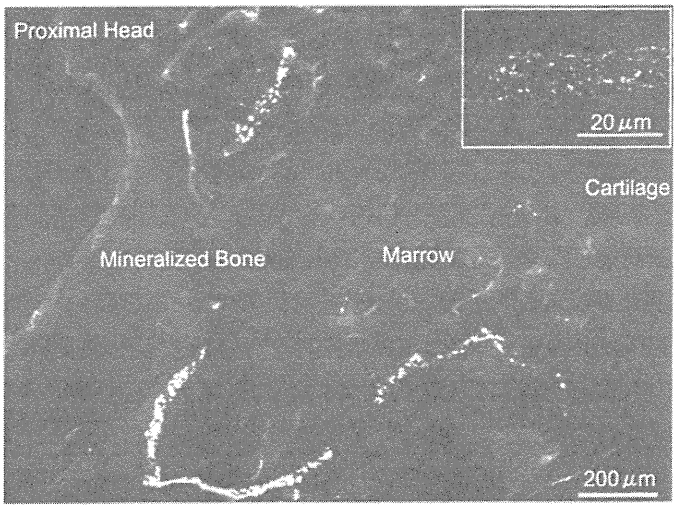

図5　骨組織内の交感神経線維の分布

骨組織内のTH陽性交感神経線維はらせん状の形態を呈して分布している。

Mineralaized Bone：皮質骨＋海綿骨，Marrow：骨髄腔，Proximal Head：大腿骨近位骨端部，TH：tyrosine hydroxylase

（文献9より引用）

をしている[11)12)]。骨組織内のtyrosine hydroxylase（TH）陽性の交感神経線維はらせん状の形態を呈しており，ほかの知覚神経線維が直線状の形態を呈することと比較して特徴的である[9)]。これはハバース管内を通る血管を取り巻くように分布しているためと考えられている（図5）。交感神経の分布密度は骨膜と皮質骨・海綿骨では遠位骨端部が高く，骨髄腔では近位骨端部が高いとされている[9)]。

骨の疼痛発症メカニズム

近年，骨性疼痛の発症メカニズムに関する研究が進んでいる。とくに，がんの骨転移[13)]や骨粗鬆症[14)]，骨Paget病[15)]などの骨吸収亢進状態を呈する疾患において骨性の疼痛を伴うことがわかってきた。これらの疾患では，破骨細胞の活性化に伴う骨吸収亢進状態を呈している。骨吸収亢進に伴

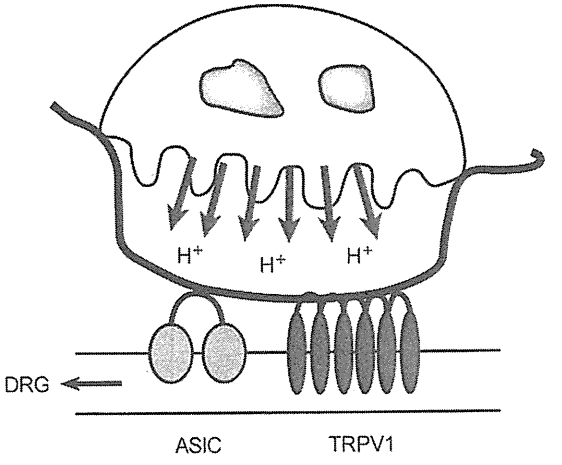

図6　骨吸収亢進状態における疼痛発症メカニズム

破骨細胞が産生する酸がTRPV1やASICなどの酸受容体を介して骨に分布する侵害受容性神経を興奮させることにより痛みを引き起こす。

DRG：後根神経節

（文献7，17より改変引用）

TH：tyrosine hydroxylase

い，破骨細胞が産生する酸が増加して局所のpHが低下する。また，骨組織内には酸受容体であるTRPV1（transient receptor potential channel-vanilloid subfamily member 1）やASIC（acid-sensing ion channel）が存在する[16]。これらの受容体を介して骨に分布する侵害受容性神経を興奮させて痛みを引き起こすと考えられている（図6）[17]。

卵巣摘除（OVX）マウスを用いた骨粗鬆症性疼痛の研究

現在，筆者らはOVXマウスを用いて，骨粗鬆症に伴う疼痛の発生メカニズムについて研究を進めている。これまでに行った行動学的評価や免疫組織学的評価によると，骨粗鬆症モデル（OVX）マウスでは偽手術（sham）マウスと比較して疼痛閾値の有意な低下を呈した（図7）。また，一次求心性神経からの侵害信号が入力される脊髄後角でc-Fosの発現増強を認めた。c-Fosは痛み刺激による脊髄後角ニューロンの活性化指標として用いられる。さらに，興味深いことに，破骨細胞機能を抑制する骨吸収抑制剤のビスホスホネート（BP）を投与すると，低下した疼痛閾値の改善を認めた（図7）。このことは骨組織内の侵害受容性神経に存在する酸受容体が活性化して疼痛を引き起こしていることを示唆している。

一方，最近の研究結果では，骨粗鬆症モデルマウスで誘発された疼痛域値低下がTRPV1拮抗薬を用いても改善することが明らかとなった。しか

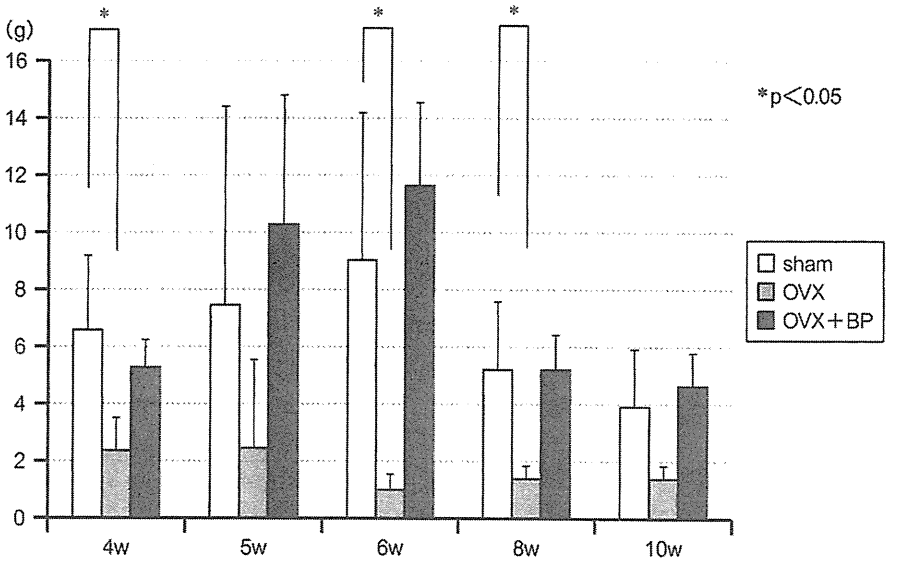

図7　骨粗鬆症モデルマウスにおける疼痛域値の変化

骨粗鬆症（OVX）群は偽手術（sham）群と比較して疼痛域値の有意な低下を認め，さらにビスホスホネート（BP）投与で疼痛域値の改善を認めた。OVX後4，5，6，8，10週後にvon Frey testによる疼痛行動評価を行った。また，sham群，OVX後にBPを投与した群（OVX＋BP群）と疼痛域値を比較検討した。

（筆者ら作成）

ASIC：acid-sensing ion channel，BP：ビスホスホネート，TRPV1：transient receptor potential channel-vanilloid subfamily member 1